An Equation of State for the Thermodynamic Properties of Dimethyl Ether

Cite as: J. Phys. Chem. Ref. Data **40**, 023104 (2011); https://doi.org/10.1063/1.3582533
Submitted: 11 January 2011 . Accepted: 31 March 2011 . Published Online: 08 June 2011

Jiangtao Wu (吴江涛), Yong Zhou (周永), and Eric W. Lemmon

An Equation of State for the Thermodynamic Properties of Dimethyl Ether

Jiangtao Wu (吴江涛)[a] and **Yong Zhou** (周永)

State Key Laboratory of Multiphase Flow in Power Engineering, Xi'an Jiaotong University, Xi'an Shaanxi 710049, People's Republic of China

Eric W. Lemmon

Thermophysical Properties Division, National Institute of Standards and Technology, 325 Broadway, Boulder, Colorado 80305, USA

(Received 11 January 2011; accepted 31 March 2011; published online 8 June 2011)

A thermodynamic property formulation for dimethyl ether has been developed based on a selection of experimental thermodynamic property data. The formulation includes a fundamental equation, a vapor-pressure equation, and saturated-density equations for liquid and vapor states. In determining the coefficients of the equation of state, multi-property fitting methods were used that included single-phase pressure-density-temperature ($p\rho T$), heat capacity, vapor pressure, and saturated density data. Deviations between experimental and calculated data are generally within the experimental accuracy. The equation of state has been developed to conform to the Maxwell criterion for two-phase liquid-vapor equilibrium states, and is valid for temperatures from the triple-point temperature to 550 K, with pressures up to 50 MPa and densities up to 19 mol dm^{-3}. The uncertainties of the equation of state in density are 0.1% for the liquid phase and 0.3% for the vapor phase. In the extended critical region, the uncertainties in density are 0.5%, except for very near the critical point. The uncertainties in vapor pressure are 0.2% above 230 K, and increase as temperature decreases. The uncertainties in saturated liquid density are 0.05%, except for near the critical point. The uncertainties in heat capacity are 2.0%. Detailed comparisons between the experimental data and calculated values are given. © *2011 American Institute of Physics*. [doi:10.1063/1.3582533]

Key words: correlation; dimethyl ether; equation of state; thermodynamic properties.

CONTENTS

List of Tables

List of Figures

[a]Author to whom correspondence should be addressed. Electronic mail: jtwu@mail.xjtu.edu.cn; Fax: 86-29-82668789.

List of Symbols

a_i, n_i, v_i = Coefficients
B = Second virial coefficient
C = Third virial coefficient
c_p = Isobaric heat capacity
c_v = Isochoric heat capacity
c_σ = Saturation heat capacity
d, l, t, u, β, γ, ε, η = Exponents
f = Helmholtz energy
h = Enthalpy
i, k = Serial numbers
M = Molar mass
p = Pressure
R = Molar gas constant
S = Sum of squares
s = Entropy
T = Absolute temperature
v = Molar volume
W = Statistical weight
w = Sound speed
Z = Compressibility factor

Greek Letters

Δ = Deviation
δ = Reduced density
φ = Dimensionless Helmholtz energy
θ = Functions
ρ = Molar density
τ = Inverse reduced temperature
ω = Acentric factor

Superscripts

o = Ideal gas
r = Residual
′ = Saturated-liquid state
″ = Saturated-vapor state

Subscripts

0 = Reference-state property
c = Critical
calc = Calculated
expt = Experimental
l = Liquid property
nbp = Normal-boiling-point property
tp = Triple-point property
v = Vapor property
σ = Saturation property

1. Introduction

Dimethyl ether ($(CH_3)_2O$, RE-170) is the simplest ether and is a colorless gas at atmospheric conditions. The physical

TABLE 1. Physical constants and characteristic properties of dimethyl ether

Symbol	Quantity	Value
R	Molar gas constant	8.314 472 J mol^{-1} K^{-1}
M	Molar mass	46.068 44 g mol^{-1}
T_c	Critical temperature	400.378 K
p_c	Critical pressure	5336.8 kPa
ρ_c	Critical density	5.940 mol dm^{-3}
T_{tp}	Triple-point temperature	131.66 K
p_{tp}	Triple-point pressure	2.2 Pa
ρ_{tpv}	Vapor density at the triple point	2.020×10^{-6} mol dm^{-3}
ρ_{tpl}	Liquid density at the triple point	19.150 mol dm^{-3}
T_{nbp}	Normal-boiling-point temperature	248.368 K
ρ_{nbpv}	Vapor density at the normal boiling point	0.0510 mol dm^{-3}
ρ_{nbpl}	Liquid density at the normal boiling point	15.958 mol dm^{-3}
ω	Acentric factor	0.196
T_0	Reference temperature for ideal-gas properties	273.15 K
p_0	Reference pressure for ideal-gas properties	1.0 kPa
h_0^o	Reference ideal-gas enthalpy at T_0	23242.00 J mol^{-1}
s_0^o	Reference ideal-gas entropy at T_0 and p_0	131.3883 J mol^{-1} K^{-1}

characteristics and properties of dimethyl ether are given in Table 1. Dimethyl ether is an important raw material that is widely used for pharmaceutical, alternative fuel, pesticide, and chemical applications. It is useful as a precursor to other organic compounds and as an aerosol propellant. Since the last century, researchers have found that dimethyl ether has excellent combustion characteristics, and mixtures with it can replace diesel as a fuel; dimethyl ether produces minimal NO_x and CO when combusted, and the use of dimethyl ether as a fuel additive has been extensively investigated.[1] In addition, dimethyl ether is a potential green refrigerant with an ozone depletion potential equal to 0, and a global warming potential equal to 0.1 (over 100 years, $CO_2=1$).[2] At present, dimethyl ether is produced primarily by converting hydrocarbons, predominantly from natural gas.

The thermophysical properties of dimethyl ether are very important, and many researchers have measured its properties. In recent years, the authors' groups have launched a systematic study on the thermophysical properties of dimethyl ether. At present, we have acquired much experimental data for this fluid, such as the critical parameters, saturated-vapor densities, saturated-liquid densities, vapor pressures, pvT properties, and so on.[3–11]

Ihmels and Lemmon[12] developed a fundamental equation of state for dimethyl ether in 2007. Their equation is a ten-term equation explicit in the Helmholtz energy without Gaussian bell-shaped terms. The equation is valid from the triple-point temperature (131.66 K) to 525 K, with pressures up to 40 MPa and densities up to 19 mol dm^{-3}. Many experimental data have been published since the equation was developed, hence the equation of state for dimethyl ether needs to be updated. Comparisons of the two equations of state were performed.

The purpose of this work is to develop the auxiliary equations and the equation of state for dimethyl ether on the basis of an extensive collection of experimental data.

2. Critical and Triple Parameters of Dimethyl Ether

The critical parameters are important fundamental properties for the fluid and are a prerequisite for the development of the auxiliary equations and equation of state. The authors launched a search on the existing critical parameters of dimethyl ether and found that the differences between these data are significant. Detailed information can be found in Table 2 (temperatures are converted to ITS-90) and Figs. 1–3.

It is difficult to determine the critical parameters. As described in detail in Wu's Ph.D. dissertation,[3] there are shortcomings and faults in the classical methods for determining the critical parameters. After comprehensive analysis and evaluation, we used the critical temperature $T_c=(400.378\pm0.01)$ K that was determined by the authors' groups previously.[3,6] It is difficult to accurately determine the critical density because of the infinite compressibility at the critical point and the difficulty of reaching thermodynamic equilibrium. The critical density was determined to be (5.94 ± 0.25) mol dm^{-3} during the fitting process of the equation of state. The critical pressure was determined from the final equation of state as a calculated point at the critical temperature and density—the value is (5336.8 ± 50) kPa. Figures 1–3 show the critical temperature, density, and pressure as functions of the year that they were reported.

The triple-point temperature of dimethyl ether was measured by Kennedy *et al.*[13] with a reported value of 131.66 K. Since the triple-point pressure is too small to be measured directly, it was calculated to be 2.2 Pa from the final equation of state. The other fundamental constants are given in Table 1.

3. Auxiliary Equations

The auxiliary equations include the vapor-pressure equation and the saturated-density equations for liquid and vapor states. The properties along the saturation lines can be calculated quickly and expediently through them. In order to keep consistency over the whole thermodynamic surface, the properties must be calculated with the equation of state. At saturation, application of the so-called Maxwell criteria is needed, which includes an iteration procedure. These criteria require equal Gibbs energies and equal pressures for the saturated-liquid and vapor states at the same temperature. The auxiliary equations are not required, but they can be used to calculate the initial value for the iteration to speed up the calculation.

3.1. The vapor-pressure equation

Table 3 summarizes the available experimental vapor-pressure data for dimethyl ether. There are at least 42 vapor-pressure data sets for dimethyl ether, but most of them deviate significantly from each other. As the experimental data at

TABLE 2. Published critical parameters of dimethyl ether

Year	Authors	Critical Temperature (K)	Critical Pressure (kPa)	Critical Density (mol dm^{-3})	Data Type
1883	Nadezhdin[31]	402.8			Experimental
1897	Ledue and Sacerdote[32]		5800		Experimental
1907	Briner and Cadoso[33]	400	5400		Experimental
1908	Briner and Cadoso[34]	400.2	5400		Experimental
1923	Cardoso and Bruno[35]	400.0	5270		Experimental
1923	Cardoso and Coppola[36]			5.891	Experimental
1932	Winkler and Maass[37]	399.4	5400		Experimental
1933	Winkler and Maass[38]	399.6			Experimental
1933	Tapp *et al.*[39]	400.0		4.895	Experimental
1935	Edwards and Maass[40]	400.0	5330	5.351	Experimental
1936	Pall and Maass[41]	400.0			Experimental
1970	Oshipiuk and Stryjek[42]	400			Experimental
1970	Zawisza and Glowka[43]	400.3	5359	6.100	Experimental
1991	Noles and Zollweg[44]	399.40	5270		Experimental
1992	Noles and Zollweg[45]	399.4	5264		Experimental
2001	Kudchadker *et al.*[46]	400.2	5340	5.969	Recommended
2004	Wu *et al.*[5]	400.378	5355.8		Experimental
2004	Wu *et al.*[6]	400.378	5356	5.904	Experimental
2005	Tsuji[a]	399.60	5293	6.265	Estimated
2005	Yasumoto *et al.*[47]	399.63	5268	5.883	Experimental
2007	Ihmels and Lemmon[12]	400.3	5340.5	6.013	Experimental
2008	Wu and Yin[10]		5335.1		Estimated
2011	**This work**	**400.378 ± 0.01**	**5336.845 ± 50**	**5.94 ± 0.25**	**Estimated**

[a]Reported in the work of Yasumoto *et al.*[47]

low temperatures are very limited and scattered, the data evaluated from measured isochoric heat capacities in the vapor-liquid region by Wu and Magee[8] were used, from a method for evaluating vapor pressure from internal energy measurements proposed by Duarte-Garza and Magee.[14] A new vapor-pressure equation for dimethyl ether has been correlated with the Wagner equation in the "2.5, 5" form.[15] The equation is given by

$$\ln\left(\frac{p_\sigma}{p_c}\right) = \frac{T_c}{T}(n_1\theta + n_2\theta^{1.5} + n_3\theta^{2.5} + n_4\theta^5), \quad (1)$$

where $n_1 = -7.112\,782$, $n_2 = 1.971\,239$, $n_3 = -2.276\,083$, $n_4 = -2.215\,774$, $\theta = (1 - T/T_c)$, and p_σ is the vapor pressure. The values of the critical parameters are given in Table 1.

3.2. The saturated-liquid density equation

The experimental saturated-liquid density data are summarized in Table 4. The data reported by Maass and Boomer[16]

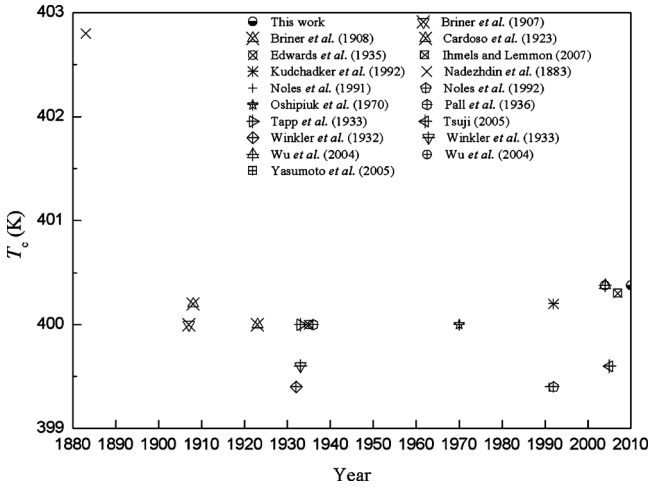

FIG. 1. Reported critical temperatures T_c of dimethyl ether as a function of the year published.

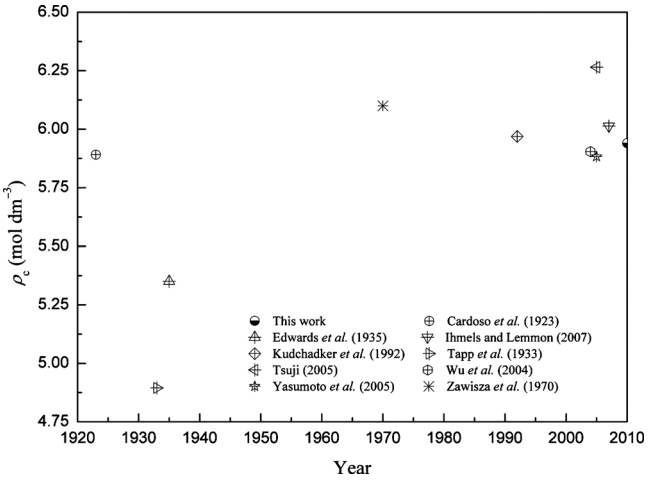

FIG. 2. Reported critical densities ρ_c of dimethyl ether as a function of the year published.

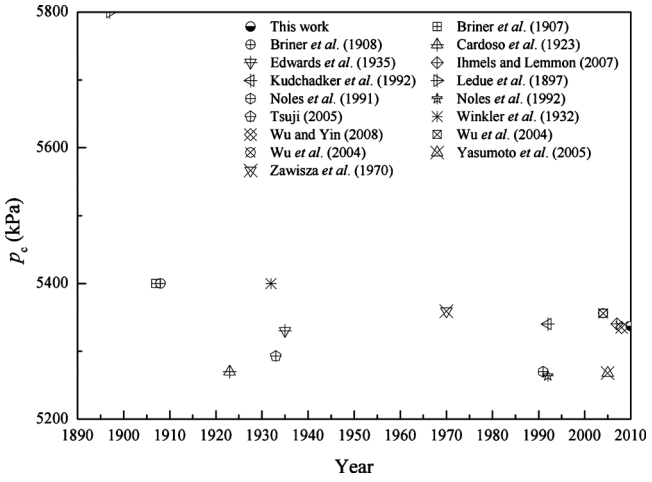

FIG. 3. Reported critical pressures p_c of dimethyl ether as a function of the year published.

are quite old (1922), and the uncertainty of the data reported by Wu *et al.*[4] is about 0.1 mol dm^{-3}. Hence, neither source was used to develop the new saturated-liquid density equation. The data reported by Wu and Magee[8] and the values generated by the final equation of state of this work from 346 to 400 K were used to correlate the saturated-liquid density equation by use of the simplex method.[17] The saturated-liquid density can be represented by

$$\frac{\rho'}{\rho_c} = 1 + n_1\theta^{0.54} + n_2\theta^{0.74} + n_3\theta^{0.95} + n_4\theta^{11.43}, \quad (2)$$

where $n_1=7.884\,834$, $n_2=-10.516\,328$, $n_3=5.391\,42$, $n_4=0.404\,890$, $\theta=(1-T/T_c)$, and ρ' is the saturated-liquid density.

TABLE 3. Summary of vapor-pressure data for dimethyl ether

Year	Authors	Number of data (used)	Temperature range (K)	AAD (%)	Bias (%)
1922	Maass and Boomer[16]	21	206–249	1.94	−1.91
1923	Cardoso and Bruno[35]	23	273–400	1.00	−0.372
1941	Kennedy *et al.*[13]	16	172–248	1.71	1.71
1972	Glowka[48]	3	323–363	0.597	−0.400
1981	Tsang and Streett[49]	9	273–387	1.47	−1.44
1982	Chang *et al.*[50]	7	273–393	1.63	−0.212
1984	Preuss and Moerke[51]	3	288–308	0.179	−0.179
1986	Calado *et al.*[52]	1	182	0.643	0.643
1988	Holldorff and Knapp[53]	19	254–320	0.091	0.089
1991	Noles and Zollweg[44]	3	283–363	0.449	0.032
1991	Preuss *et al.*[54]	2	333–373	0.063	−0.063
1992	Noles and Zollweg[45]	6	283–395	0.387	0.387
1992	Pozo de Fernandez *et al.*[55]	8	283–387	0.265	0.168
1992	Tsujimoto *et al.*[56]	22	283–393	0.247	0.139
1995	Jonasson *et al.*[57]	3	288–316	1.72	1.72
1995	Jonasson *et al.*[58]	14	274–393	0.909	0.173
1998	Bobbo *et al.*[2]	2	303–323	0.182	−0.182
2000	Bobbo *et al.*[59]	4	280–320	0.164	−0.164
2000	Bobbo *et al.*[60]	3	283–313	0.190	−0.045
2000	Giles and Wilson[61]	2	273–323	0.211	−0.211
2001	Teodorescu and Rasmussen[62]	4	288–353	0.495	0.495
2002	Florusse *et al.*[63]	24	288–399	0.471	0.471
2002	Bobbo *et al.*[64]	4	258–303	0.078	−0.078
2002	Laursen *et al.*[65]	5	298–320	1.19	−0.552
2003	Daiguji and Hihara[66]	10	263–383	0.105	−0.032
2004	Bobbo *et al.*[67]	3	278–308	0.250	−0.250
2004	Wu *et al.*[5]	39	233–400	1.641	1.641
2005	Bobbo *et al.*[68]	7	283–343	0.464	−0.464
2005	Fedele *et al.*[69]	3	258–293	0.171	0.136
2005	Valtz *et al.*[70]	27	278–361	0.190	−0.190
2006	Corvaro *et al.*[71]	70	219–361	0.448	−0.035
2006	Im *et al.*[72]	6	313–363	0.476	0.177
2007	Ihmels and Lemmon[12]	19 (19)	264–397	0.111	−0.009
2007	Im *et al.*[73]	6	313–363	0.486	0.383
2007	Park *et al.*[74]	6	323	0.063	−0.020
2008	Wu and Yin[10]	39 (31)	213–393	0.267	0.200
2009	Wu and Magee[8]	150(150)	132–280	0.062	0.005
2010	Tanaka and Higashi[29]	6	310–360	0.121	0.034

TABLE 4. Summary of saturated-liquid density data for dimethyl ether

Year	Authors	Number of data (used)	Temperature range (K)	AAD (%)	Bias (%)
1922	Maass and Boomer[16]	11	232–261	0.135	−0.076
1923	Cardoso and Coppola[36]	12	273–400	1.201	−1.201
1936	Pall and Maass[41]	26	287–393	0.245	−0.245
1940	Grosse *et al.*[75]	12	193–273	0.398	−0.398
1951	De Mallemann *et al.*[76]	2	198–250	0.323	−0.221
1986	Calado *et al.*[52]	1	182	0.116	0.166
2003	Wu *et al.*[4]	24	227–342	0.936	−0.936
2003	Wu *et al.*[7]	31	213–368	0.115	0.115
2004	Wu *et al.*[5]	18	302–400	0.807	0.487
2005	Bobbo *et al.*[68]	7	283–343	0.116	0.081
2006	Wu *et al.*[9]	9	233–323	0.488	−0.384
2009	Wu and Magee[8]	91(91)	133–345	0.004	0.002
2010	Tanaka and Higashi[29]	6	310–360	0.250	−0.250

3.3. The saturated-vapor density equation

As shown in Table 5, the experimental saturated-vapor density data are limited; only 51 data points are available. Even worse, 13 of them are quite old and the rest were obtained by the same group, so that the internal consistency among different groups could not be checked. Values generated from the final equation of state in this work with the Maxwell criteria were used in developing the saturated-vapor density equation with the simplex method.[17] The saturated-vapor density can be represented by

$$\ln\left(\frac{\rho''}{\rho_c}\right) = n_1\theta^{1.467/3} + n_2\theta^{4.2/3} + n_3\theta^{8/3} + n_4\theta^{17/3} + n_5\theta^{36/3}, \tag{3}$$

where $n_1=-4.136\,444$, $n_2=-4.302\,025$, $n_3=-12.032\,140$, $n_4=-39.527\,936$, $n_5=-89.476\,860$, $\theta=(1-T/T_c)$, and ρ'' is the saturated-vapor density.

4. The Equation of State

The equation of state developed in this work is formulated by using the Helmholtz energy as the fundamental property with temperature and density as independent variables,

$$f(T,\rho) = f^o(T,\rho) + f^r(T,\rho), \tag{4}$$

where f is the Helmholtz energy, $f^o(T,\rho)$ is the ideal-gas Helmholtz energy, and $f^r(T,\rho)$ is the residual Helmholtz energy. Modern equations of state are often formulated in this way because all other thermodynamic properties can be calculated through the derivatives of the Helmholtz energy.[18,19] The dimensionless reduced Helmholtz energy becomes

$$\frac{f(T,\rho)}{RT} = \frac{f^o(T,\rho)}{RT} + \frac{f^r(T,\rho)}{RT} = \phi^o(\tau,\delta) + \phi^r(\tau,\delta), \tag{5}$$

where the inverse reduced temperature is $\tau=T_c/T$ and the reduced density is $\delta=\rho/\rho_c$.

TABLE 5. Summary of saturated-vapor density data for dimethyl ether

Year	Authors	Number of data	Temperature range (K)	AAD (%)	Bias (%)
1923	Cardoso and Coppola[36]	13	273–400	5.92	−2.46
1941	Kennedy *et al.*[13]	1	247	13.3	−13.3
2003	Wu *et al.*[7]	31	213–368	2.67	2.31
2004	Wu *et al.*[6]	7	367–400	4.38	−4.38

4.1. Ideal-gas Helmholtz energy

The ideal-gas Helmholtz energy, in dimensionless form, can be represented by

$$\phi^o(\tau,\delta) = \frac{h_0^o\tau}{RT_c} - \frac{s_0^o}{R} - 1 + \ln\frac{\delta\tau_0}{\delta_0\tau} - \frac{\tau}{R}\int_{\tau_0}^{\tau}\frac{c_p^0}{\tau^2}d\tau + \frac{1}{R}\int_{\tau_0}^{\tau}\frac{c_p^0}{\tau}d\tau, \tag{6}$$

where c_p^0 is the ideal-gas heat capacity, $\tau_0=T_c/T_0$, $\delta_0=\rho_0/\rho_c$, and ρ_0 is the ideal-gas density, which can be calculated by the ideal-gas equation of state ($\rho_0=p_0/RT_0$). The parameters T_0, p_0, ρ_0, h_0^o, and s_0^o are arbitrary constants that are used to set the enthalpy and entropy to a prescribed reference state. As shown in the above equations, the ideal-gas heat capacity c_p^0 is used to calculate the ideal-gas Helmholtz energy. The ideal-gas heat capacity c_p^0 can be obtained by statistical methods or by correlating experimental data. In general, all fluids can be fitted with the same functional form,[18]

$$\frac{c_p^0}{R} = c_0 + \sum_{k=1}^{4} v_k\left(\frac{u_k}{T}\right)^2\frac{\exp(u_k/T)}{(\exp(u_k/T)-1)^2}, \tag{7}$$

where $R=8.314\,472$ J mol^{-1} K^{-1} is the molar gas constant.[20] Since there are no new precise data available, the equation developed by Ihmels and Lemmon[12] was selected; the coefficients and exponents are $c_0=4.039$, $u_1=361$ K, $u_2=974$ K,

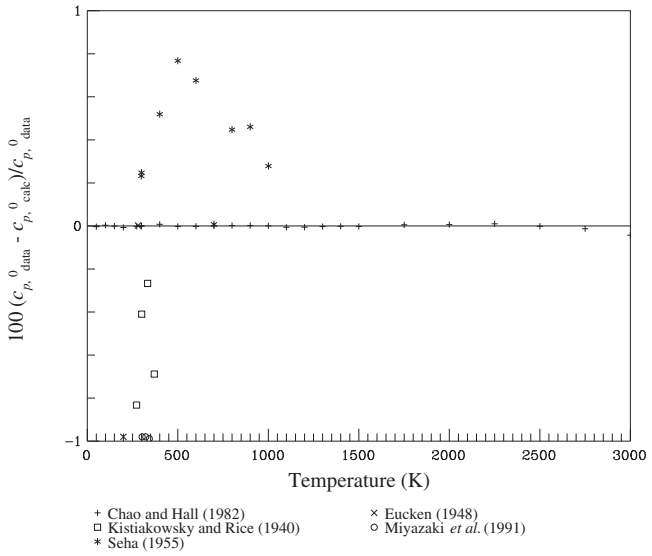

FIG. 4. Comparisons of ideal gas heat capacities c_p^0 calculated with Eq. (7) to experimental and theoretical data as a function of temperature.

$u_3=1916$ K, $u_4=4150$ K, $v_1=2.641$, $v_2=2.123$, $v_3=8.992$, and $v_4=6.191$. Figure 4 shows comparisons of ideal-gas heat capacities c_p^0 calculated by Eq. (7) to experimental and theoretical data as a function of temperature T.

The ideal-gas Helmholtz energy equation, derived from Eqs. (6) and (7), is

$$\phi^0 = a_1 + a_2\tau + \ln\,\delta + (c_0 - 1)\ln\,\tau + \sum_{k=1}^{4} v_k \ln[1 - \exp(-u_k\tau/T_c)], \tag{8}$$

where

$$a_1 = -1 + \ln(\tau_0/\delta_0) + c_0 - c_0 \ln\,\tau_0 - \frac{s_0^o}{R} - \sum_{k=1}^{4} v_k \left[\frac{u_k\tau_0/T_c}{1 - \exp(u_k\tau_0/T_c)} + \ln(1 - \exp(-u_k\tau_0/T_c))\right] = -1.980\,976, \tag{9}$$

and

$$a_2 = \frac{h_0^o}{RT_c} - \frac{c_0}{\tau_0} - \sum_{k=1}^{4} v_k \frac{u_k/T_c}{\exp(u_k\tau_0/T_c) - 1} = 3.171\,218. \tag{10}$$

The ideal-gas reference state points are $T_0=273.15$ K, $p_0=1.0$ kPa, $h_0^o=23\,242.00$ J mol^{-1}, and $s_0^o=131.3883$ J mol^{-1} K^{-1}. The values for h_0^o and s_0^o were chosen so that the enthalpy and entropy of the saturated liquid state at the normal boiling point are 0 kJ kg^{-1} and 0 kJ kg^{-1} K^{-1}, respectively. Other reference states can also be used. The values of the other coefficients are the same as used in Eq. (7).

4.2. Residual Helmholtz energy

Unlike the ideal-gas Helmholtz energy equation, the residual Helmholtz energy equation is fitted with large numbers of multiproperty experimental data, such as $p\rho T$, heat capacity, sound speed, vapor pressure, saturated-liquid density, and saturated-vapor density. The authors have summarized the available experimental data of dimethyl ether, which are listed in Tables 3–7. The data finally used in fitting the equation of state are also marked in the tables.

In this work, the nonlinear fitting algorithm used to optimize the residual Helmholtz energy equation was based on the Levenberg–Marquardt method.[21] The fitting algorithm minimizes the function

$$S = \sum W_\rho \left[\frac{(\rho_{\text{expt}} - \rho_{\text{calc}})}{\rho_{\text{expt}}}\right]^2 + \sum W_p \left[\frac{(p_{\text{expt}} - p_{\text{calc}})}{\rho_{\text{expt}}}\left(\frac{\partial\rho}{\partial p}\right)\right]^2 + \sum W_{c_v} \left[\frac{(c_{v,\text{expt}} - c_{v,\text{calc}})}{c_{v,\text{expt}}}\right]^2 + \cdots, \tag{11}$$

where W specifies the weight assigned to a particular property. A different weight W was assigned to each data point used in the fitting process. The quality of the resulting equation of state is determined through comparison of calculated deviations of individual data points and the total deviations of specific data sets. The final weight on a data point should reflect the approximate uncertainty. In general, data points with uncertainties less than 0.01% are given final weights of 1000, those with uncertainties less than 0.1% are given final weights of 10–100, those with uncertainties of 0.1%–0.2% are often given final weights of 1, and those with higher uncertainties are given weights of 0.01–0.1. Overall, the process of fitting the equation of state is a process of finding a balance between the weights and the reliable data.

There are some criteria for the equation of state to conform to expected behavior at experimentally accessible states and at high temperatures and pressures. The values of t_i in the equation given below should be greater than zero, and d_i and l_i should be integers greater than zero. The temperature exponent t_i on the density exponent $d_i=4$ is fixed exactly to 1 for the equation of state to have proper extrapolation behavior at high densities and temperatures—Sec. 4.4 shows that the extrapolation behavior of the equation of state is reasonable at extremely high pressures, densities, and temperatures. In addition, the number of polynomial terms used should be limited to avoid irregular behavior; in this work, only five polynomial terms are used: two to represent the second virial coefficient ($d_i=1$), one for the third virial coefficient ($d_i=2$), one for the fourth virial coefficient ($d_i=3$), and the term for the extreme conditions ($d_i=4$). The work of Lemmon and Jacobsen[22] should be consulted for more information.

In contrast to the equation of state developed by Ihmels and Lemmon,[12] the functional form used in this work

TABLE 6. Summary of $p\rho T$ and virial-coefficient data for dimethyl ether

Property	Year	Authors	Number of data (used)	Temperature range (K)	Pressure range (kPa)	AAD[a] (%)	Bias (%)
$p\rho T$	1923	Cardoso and Coppola[36]	11	329–400	1323–5344	24.2	−22.6
$p\rho T$	1933	Tapp *et al.*[39]	3	273–313	100	0.194	0.194
$p\rho T$	1940	Grosse *et al.*[75]	3	253–273	101	0.157	−0.157
$p\rho T$	1962	Tripp and Dunlap[77]	21	283–323	16–92	0.060	0.060
$p\rho T$	1963	Lawley and Sutton[78]	3	292–325	100	0.066	0.064
$p\rho T$	1970	Osipiuk and Stryjek[42]	4	298–373	100	0.155	0.155
$p\rho T$	1971	Haworth and Sutton[79]	3	298–328	100	0.066	0.066
$p\rho T$	2004	Wu *et al.*[6]	5	367–366	2927–5252	21.3	−21.3
$p\rho T$	2005	Bobbo *et al.*[68]	96	283–353	550–35500	0.093	0.068
$p\rho T$	2006	Wu *et al.*[80]	7	253–323	101	0.416	−0.130
$p\rho T$	2007	Ihmels and Lemmon[12]	417(262)	273–523	877–40000	0.134	0.111
$p\rho T$	2007	Outcalt and McLinden[25]	129(128)	270–470	974–46719	0.065	−0.056
$p\rho T$	2009	Arteconi *et al.*[26]	88	298–363	535–1743	1.90	−0.645
$p\rho T$	2009	Arteconi *et al.*[27]	138	344–393	55–4015	0.326	−0.184
$p\rho T$	2009	Wu and Magee[8]	200(142)	152–344	0.1–33761	0.053	−0.050
$p\rho T$	2010	Tanaka and Higashi[29]	22	310–360	2000–5000	0.178	−0.178
$p\rho T$	2010	Yin and Wu[11]	126 (90)	328–403	184–4733	0.106	−0.103
B	1933	Cawood and Patterson[81]	3	273–313		43.9	−43.9
B	1961	Tripp[82]	6	283–323		40.7	−40.7
B	1963	Lawley and Sutton[79]	3	292–325		15.1	−14.4
B	1970	Osipiuk and Stryjek[42]	4	298–373		40.7	−40.7
B	1971	Haworth and Sutton[79]	3	298–328		16.2	−16.2
B	1992	Tsujimoto *et al.*[56]	5	298–343		94.3	−94.3
B	2009	Arteconi *et al.*[27]	30	344–393		8.66	3.97
B	2010	Yin and Wu[11]	16	383–388		3.114	3.114
C	1992	Tsujimoto *et al.*[56]	5	298–343		70.6	70.6
C	2009	Arteconi *et al.*[27]	15	343–393		9.91	−6.34

[a]For the second and third virial coefficients, the AAD stands for average absolute difference, and the bias stands for average difference. The units for AAD and bias of B and C are $cm^3\ mol^{-1}$ and $cm^6\ mol^{-2}$, respectively.

contains additional Gaussian bell-shaped terms, which were first successfully used by Setzmann and Wagner.[21] These terms allow the equation of state of this work to have better behavior in the critical region.

Based on the collected data and the ideal-gas Helmholtz energy equation $\phi^o(\tau,\delta)$, the authors have developed the residual Helmholtz energy equation $\phi^r(\tau,\delta)$ using the fitting methods of Lemmon;[22,23] the equation is constrained by various criteria explained elsewhere in the works of Span and Wagner[24] and Lemmon and Jacobsen.[22] The form of $\phi^r(\tau,\delta)$ is as follows and the coefficients as well as the exponents are given in Table 8:

TABLE 7. Summary of caloric data for dimethyl ether

Property	Year	Authors	Number of data (used)	Temperature range (K)	Pressure range (kPa)	AAD (%)	Bias (%)
Δh_{vap}	1941	Kennedy *et al.*[13]	1	248		0.377	0.377
w	1939	Jatkar[83]	2	246–274	101	0.607	0.607
w	1957	Richardson and Tait[28]	76	289–317	3964–62156	5.39	5.39
c_σ	2009	Wu and Magee[8]	90 (79)	133–345		0.301	0.121
c_{v2}	2009	Wu and Magee[8]	90	133–345		0.679	0.621
c_p	1939	Jatkar[83]	2	298–370	99–101	7.34	−7.34
c_p	1940	Kistiakowsky and Rice[84]	4	272–370	100	4.39	−4.39
c_p	1941	Kennedy *et al.*[13]	32 (31)	137–245	Saturated liquid	0.275	0.070
c_p	1991	Miyazaki *et al.*[85]	12	303–343	200–500	2.50	−2.45
c_p	2010	Tanaka and Higashi[29]	29	310–320	2000–5000	6.77	6.77
c_v	2009	Wu and Magee[8]	117(116)	133–345	0–33760	0.452	0.235

TABLE 8. The coefficients and exponents of the equation of state

i	n_i	d_i	t_i	l_i	η_i	β_i	γ_i	ε_i
1	0.029 814 139	4	1					
2	1.435 17	1	0.4366					
3	–2.649 64	1	1.011					
4	–0.295 155 32	2	1.137					
5	0.170 356 07	3	0.45					
6	–0.946 429 18	1	2.83	2				
7	–0.099 250 514	3	1.5	2				
8	1.126 407 1	2	1.235	1				
9	–0.769 365 48	2	2.675	2				
10	–0.020 717 696	7	0.7272	1				
11	0.245 270 37	1	1.816	1				
12	1.186 343 8	1	1.783		0.965 336	1.287 19	1.277 720	0.672 698
13	–0.493 983 68	1	3.779		1.508 58	0.806 235	0.430 750	0.924 246
14	–0.163 887 16	3	3.282		0.963 855	0.777 942	0.429 607	0.750 815
15	–0.027 583 584	3	1.059		9.726 43	197.681	1.138 490	0.800 022

$$\phi^r(\tau,\delta) = \sum_{i=1}^{5} n_i \delta^{d_i} \tau^{t_i} + \sum_{i=6}^{11} n_i \delta^{d_i} \tau^{t_i} \exp(-\delta^{l_i}) + \sum_{i=12}^{15} n_i \delta^{d_i} \tau^{t_i} \exp(-\eta_i(\delta-\varepsilon_i)^2 - \beta_i(\tau-\gamma_i)^2). \quad (12)$$

4.3. Comparisons with experimental data

The experimental data available are listed in Tables 3–7, with the temperatures converted to ITS-90. The percentage deviation between the experimental data and the values calculated from the equation for any property, X, is defined as

$$\Delta X = 100\left(\frac{X_{\text{expt}} - X_{\text{calc}}}{X_{\text{expt}}}\right). \quad (13)$$

With this definition, the average absolute deviation (AAD) is defined as

$$\text{AAD} = \frac{1}{N_{\text{expt}}} \sum_{i=1}^{N_{\text{expt}}} |\Delta X_i|, \quad (14)$$

where N_{expt} is the number of data points. The bias is defined as

$$\text{Bias} = \frac{1}{N_{\text{expt}}} \sum_{i=1}^{N_{\text{expt}}} (\Delta X_i). \quad (15)$$

The AAD and bias between the experimental data and the values calculated from the equation of state are listed in the last two columns of the experimental data summary tables.

4.3.1. Comparisons with saturation thermal data

The experimental vapor-pressure data are summarized in Table 3. Comparisons of vapor pressures p_σ calculated with the equation of state to experimental data as a function of temperature T are shown in Figs. 5 and 6. The equation of state represents vapor pressures generally within 0.4%. At high temperatures, the data of Ihmels and Lemmon[12] were used in developing the equation of state, and the equation of state represents the data generally within 0.1%. At low tem-

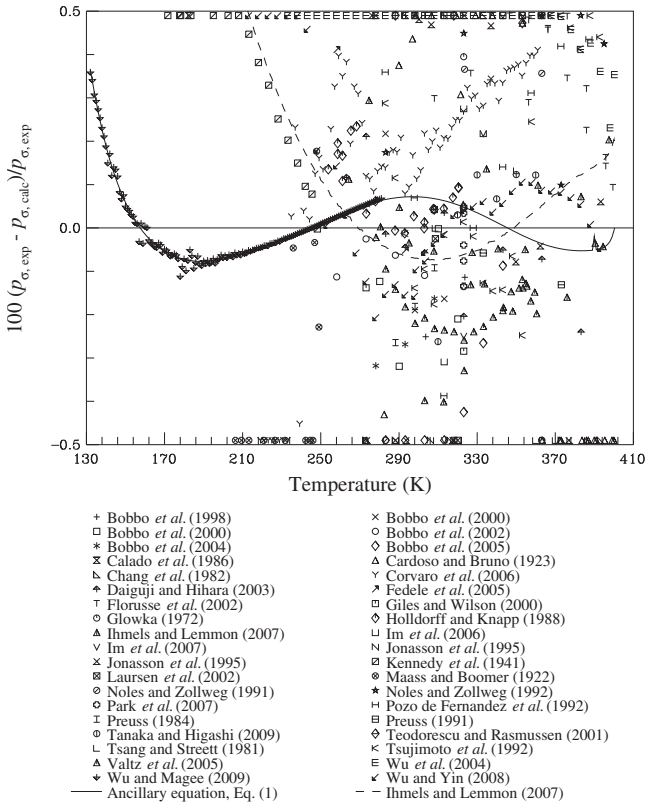

FIG. 5. Comparisons of vapor pressures p_σ calculated with the equation of state to experimental data as a function of temperature (the range of the y-axis is ±0.5%). The solid line corresponds to values calculated from the ancillary equation, Eq. (1). The dashed line corresponds to values calculated from the equation of state of Ihmels and Lemmon.[12]

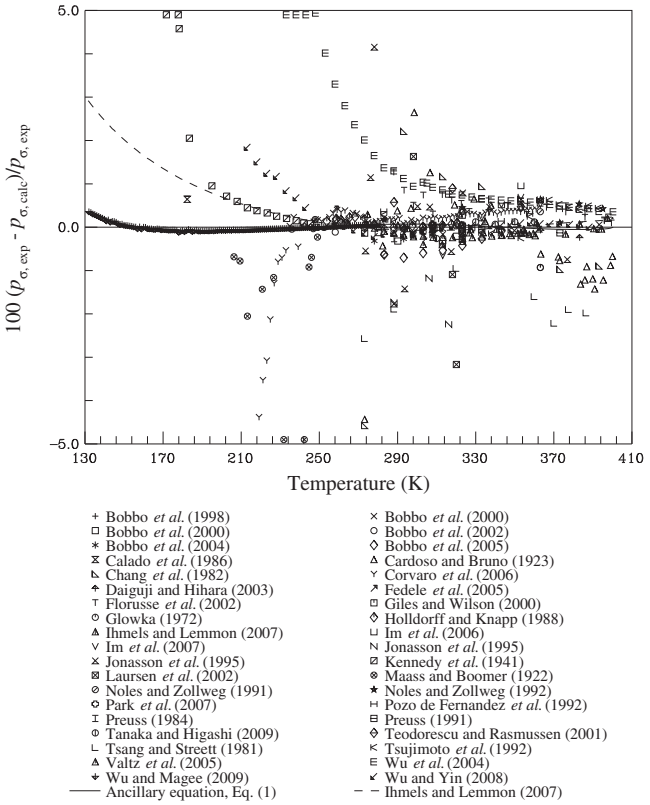

FIG. 6. Comparisons of vapor pressures p_σ calculated with the equation of state to experimental data as a function of temperature (the range of the y-axis is ±5.0%). The line corresponds to values calculated from the ancillary equation, Eq. (1). The dashed line corresponds to values calculated from the equation of state of Ihmels and Lemmon.[12]

peratures, the experimental vapor-pressure data are very limited and scattered; the data reported by different authors deviate substantially from each other, as shown in Fig. 6. Vapor pressures at low temperatures for dimethyl ether are too small to be measured precisely with experimental methods. Duarte-Garza and Magee[14] have successfully presented a method of evaluating vapor pressure from internal energy measurements. In this work, the vapor pressures at low temperatures used in developing the equation of state were evaluated from the measured isochoric heat capacity in the vapor-liquid region by Wu and Magee.[8] The equation of state represents the evaluated data generally within 0.1% in vapor pressure, and the deviations increase at lower temperatures to 0.35% near the triple point. Comparisons with the equation of Ihmels and Lemmon[12] are also shown in the plots. Their equation is very similar to the equation of this work at temperatures above 230 K, but tends to follow the data of Kennedy *et al.*[13] at lower temperatures. The data of Kennedy *et al.*[13] differ from the values derived from the data of Wu and Magee.[8]

The experimental saturated liquid densities are summarized in Table 4. The data reported by Wu and Magee[8] were used in developing the equation of state. As shown in Fig. 7, the equation of state represents the data generally within

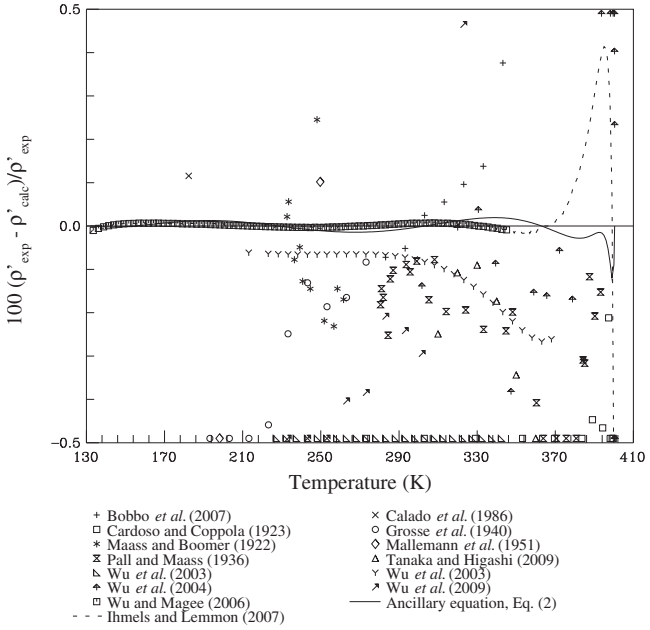

FIG. 7. Comparisons of saturated liquid densities ρ' calculated with the equation of state to experimental data as a function of temperature. The line corresponds to values calculated from the ancillary equation, Eq. (2). The dashed line corresponds to values calculated from the equation of state of Ihmels and Lemmon.[12]

0.01%. The equation of this work is very similar to the equation of Ihmels and Lemmon[12] except for the region near the critical point.

As shown in Fig. 8, the saturated-vapor density data are very scattered. None of the data were used in developing the equation of state, and the data generated from the Maxwell solution of the equation of state were used in developing the saturated-vapor density equation, Eq. (3).

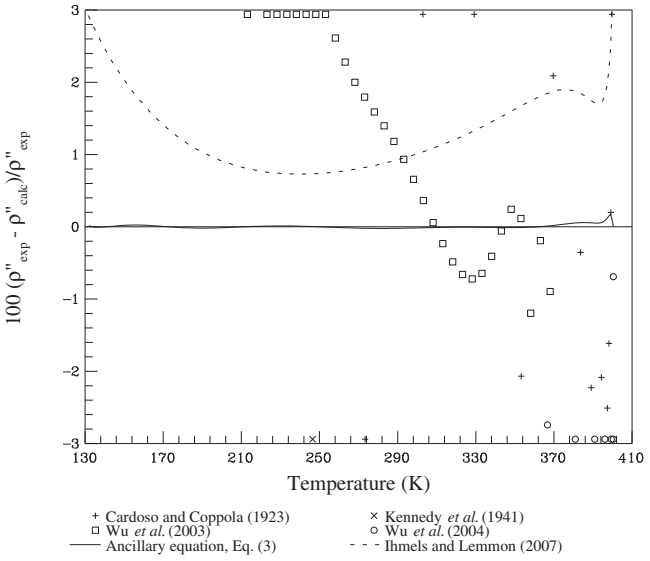

FIG. 8. Comparisons of saturated vapor densities ρ'' calculated with the equation of state to experimental data as a function of temperature. The line corresponds to values calculated from the ancillary equation, Eq. (3). The dashed line corresponds to values calculated from the equation of state of Ihmels and Lemmon.[12]

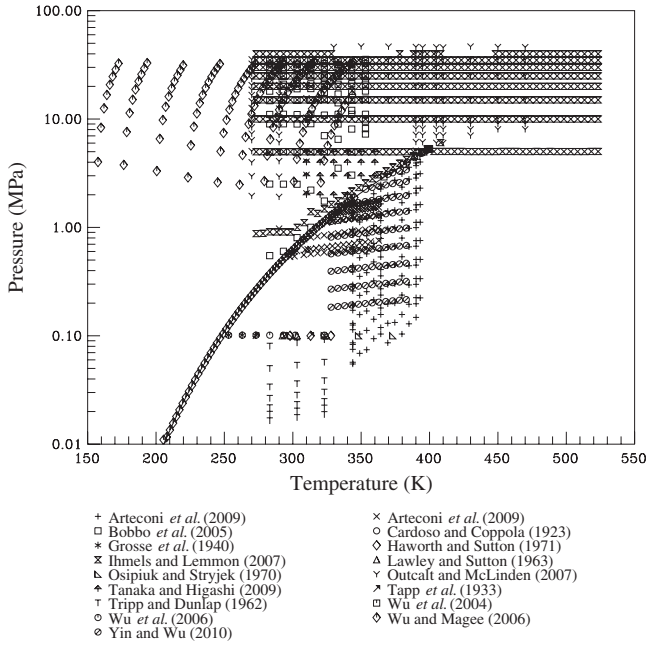

FIG. 9. Experimetal $p\rho T$ data as a function of temperature and pressure.

4.3.2. Comparisons with $p\rho T$ data and virial coefficients

The experimental $p\rho T$ data and virial coefficients are summarized in Table 6 and shown in Fig. 9. Figure 10 compares densities ρ calculated by the equation of state to experimental data as a function of pressure p; the deviations are shown in groups containing data within a 10 or 20 K interval. In the liquid phase, the data of Wu and Magee[8] and Outcalt and McLinden[25] were used in developing the equation of state at low temperatures, and the data of Outcalt and McLinden and Ihmels and Lemmon[12] were used to develop the equation of state at high temperatures, as it is very hard to judge which is more accurate. In the gas phase, the data of Yin and Wu[11] were used for developing the equation of state because the data of Arteconi *et al.*[26,27] have higher uncertainties. In the critical region, the data of Outcalt and McLinden[25] were used to develop the equation of state, as the uncertainties of the data reported by Ihmels and Lemmon[12] are larger in the critical region. Comparisons with the equation of Ihmels and Lemmon[12] are also shown in the plot. The two equations are very similar in the compressed-liquid region. In the gas region, the equation of Ihmels and Lemmon[12] deviates from the experimental data, with decreasing errors as the pressure decreases. In the critical region, the uncertainties of both equations are higher, but the equation of this work is more reasonable, as the new equation contains additional Gaussian bell-shaped terms with coefficients fitted to data and constrained to new methods described by Lemmon *et al.*[22,23]

The equation of state represents the data of Wu and Magee[8] with an AAD of 0.052%, the data of Outcalt and McLinden[25] with an AAD of 0.065%, the data of Ihmels and Lemmon[12] with an AAD of 0.134%, and the data of Yin and Wu[11] with an AAD of 0.106%. The reason for the higher AAD of the data reported by Ihmels and Lemmon[12] is that

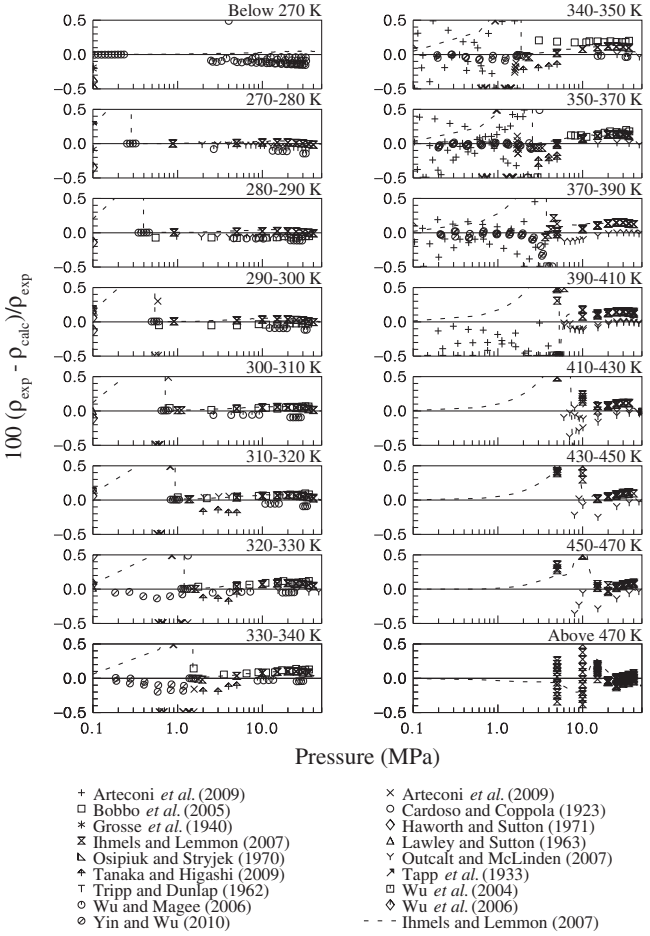

FIG. 10. Comparisons of densities ρ calculated with the equation of state to experimental data as a function of pressure. The dashed line corresponds to values calculated from the equation of state of Ihmels and Lemmon.[12]

deviations between the experimental data and the values calculated with the equation of state in the critical region are as large as 10%.

The reported data for the second virial coefficients and third virial coefficients are summarized in Table 6. Comparisons of values calculated from the equation of state are shown for the second virial coefficient in Fig. 11, and for the third virial coefficient in Fig. 12. The scatter in the virial coefficients is high, and the values were not used for developing the equation of state. The deviations show a downward trend below 300 K. The same trend is found in the analysis of Yin and Wu.[11] Figure 13, in which the y intercept (zero density) represents the second virial coefficient at a given temperature, and the third virial coefficient can be taken from the slope of each line at zero density, shows that the behavior of the second and third virial coefficients as well as the shape of the equation of state in the two-phase region are reasonable.

4.3.3. Comparisons with caloric data

The caloric data for dimethyl ether are summarized in Table 7 and shown in Fig. 14. There is only one data point for the enthalpy of vaporization of dimethyl ether. The de-

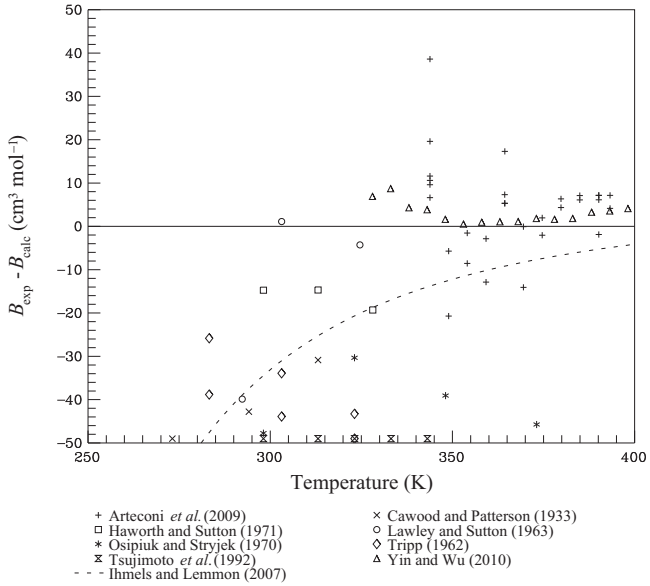

FIG. 11. Comparison of second virial coefficients B calculated with the equation of state to experimental data as a function of temperature. The dashed line corresponds to values calculated from the equation of state of Ihmels and Lemmon.[12]

viation between the point and the value calculated from the equation of state is 0.38%. There are two data sets for the sound speed for dimethyl ether. The high deviations of the data by Richardson and Tait[28] show that the data might be suspect, and these data were not used in fitting.

For the saturation heat capacity, only the data set reported by Wu and Magee[8] is available, which is summarized in Table 7. Figure 15 compares saturation heat capacities c_σ calculated with the equation of state to experimental data as a function of temperature. The deviations are generally within 1.0%, and the average absolute deviation is 0.3%. The

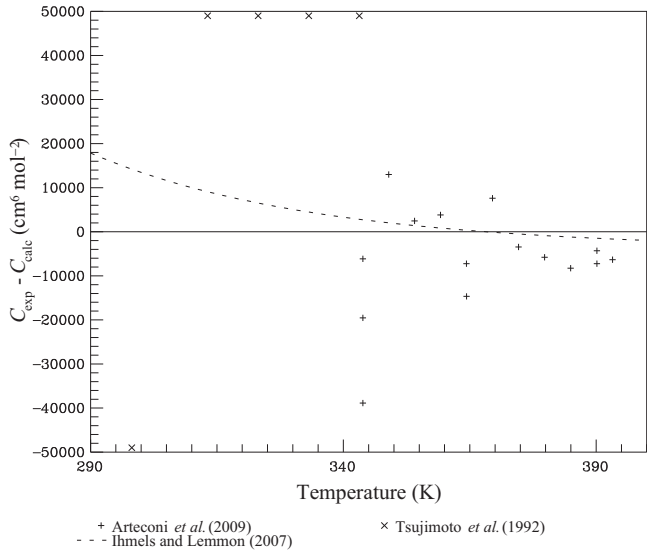

FIG. 12. Comparison of third virial coefficients C calculated with the equation of state to experimental data as a function of temperature. The dashed line corresponds to values calculated from the equation of state of Ihmels and Lemmon.[12]

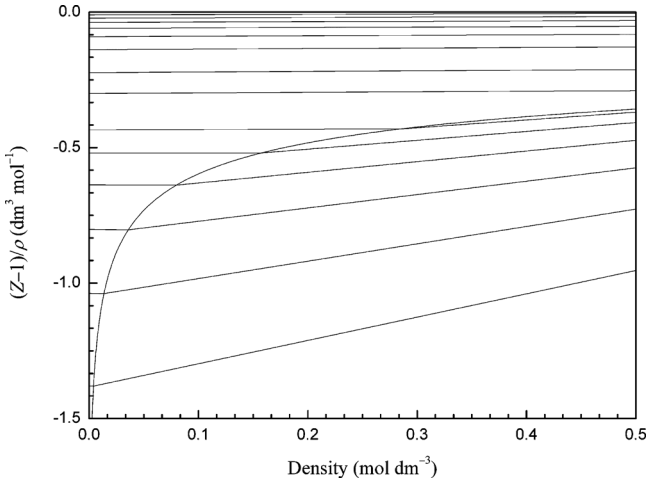

FIG. 13. Calculations of $(Z-1)/\rho$ along isotherms versus density ρ in the vapor-phase region and two-phase region. Isotherms are shown at temperatures of 220, 240, 260, 280, 300, 400.378, 500, 600, 700, 800, 900, and 1000 K.

data of Wu and Magee[8] were also used to evaluate the vapor pressure at low temperatures with the method of Duarte-Garza and Magee.[14] Two-phase isochoric heat capacities c_{v2} calculated with the equation of state are compared to experimental data as a function of temperature in Fig. 16. The average absolute deviation of the equation from the data is 0.68%. There is an upward trend in the deviations above 270 K.

The data available for the isobaric heat capacity are summarized in Table 7. They are very scattered and were not used in developing the equation of state except for the data reported by Kennedy *et al.*[13] As shown in Fig. 17, the deviations of the data of Kennedy *et al.*[13] are generally less than 1.0%, except for one data point. The data of Tanaka and Higashi,[29] which also were not used for developing the equation of state, show positive deviations of 6.5%. The rest of

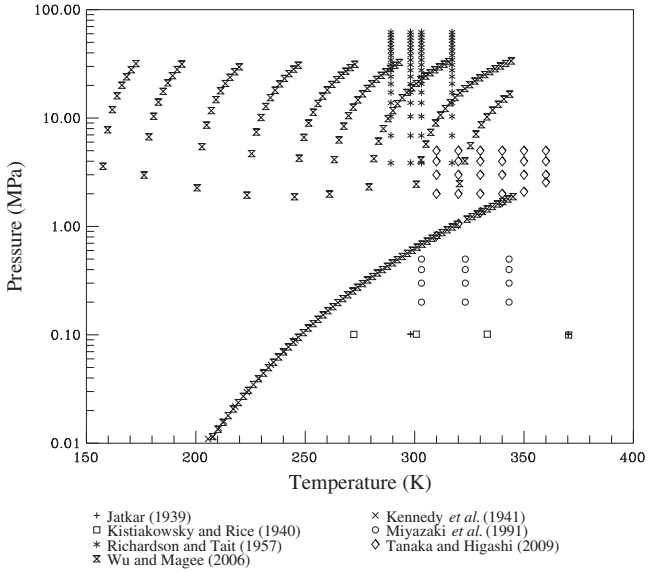

FIG. 14. Experimental caloric data as a function of temperature and pressure.

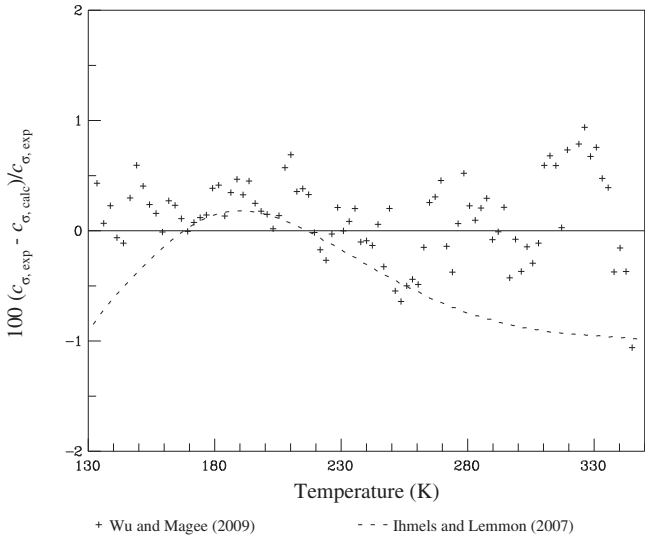

FIG. 15. Comparisons of saturation heat capacities c_σ calculated with the equation of state to experimental data as a function of temperature. The dashed line corresponds to values calculated from the equation of state of Ihmels and Lemmon.[12]

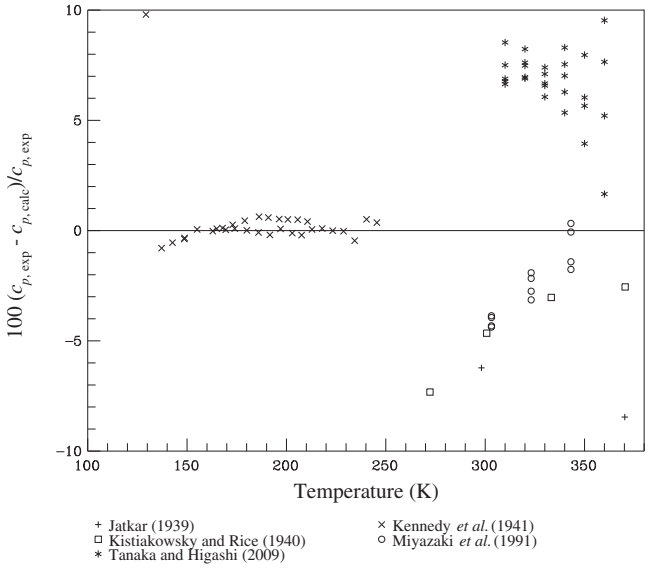

FIG. 17. Comparisons of isobaric heat capacities c_p calculated with the equation of state to experimental data as a function of temperature.

the available data show negative deviations of 2.5% or more. Overall, the situation for the isobaric heat capacity for dimethyl ether is not good, and additional measurements are needed. As summarized in Table 7, only Wu and Magee[8] reported isochoric heat capacities of dimethyl ether. The absolute average deviation of the equation from the data is 0.45%, and the equation of state represents the data within 1.0%, as shown in Fig. 18.

4.4. The extrapolation behavior of the equation of state

The equation of state should have reasonable extrapolation behavior, and a plot of constant property lines on various thermodynamic coordinates is useful in assessing the behavior. The equation developed in this work was used to plot isochoric heat capacity (Fig. 19), isobaric heat capacity (Fig. 20), and sound speed (Fig. 21) versus temperature, temperature versus density (Fig. 22), pressure versus density (Fig. 23), and characteristic (ideal) curves of the equation of state (Fig. 24).

Figure 19 shows a diagram for isochoric heat capacity c_v versus temperature. Figure 20 is a diagram for isobaric heat capacity c_p versus temperature. Both figures indicate that the equation-of-state behavior is appropriate within the valid range, and that the extrapolation behavior is reasonable at higher temperatures and pressures. In addition, Figs. 19 and 20 show that there is a reasonable upward trend in the liquid region at low temperatures below the triple-point temperature (the dashed line),[23] as expected.

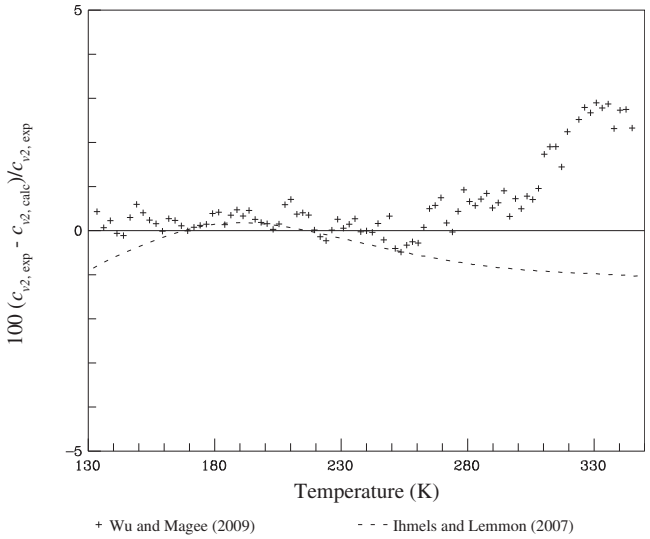

FIG. 16. Comparisons of two-phase isochoric heat capacities c_{v2} calculated with the equation of state to experimental data as a function of temperature. The dashed line corresponds to values calculated from the equation of state of Ihmels and Lemmon.[12]

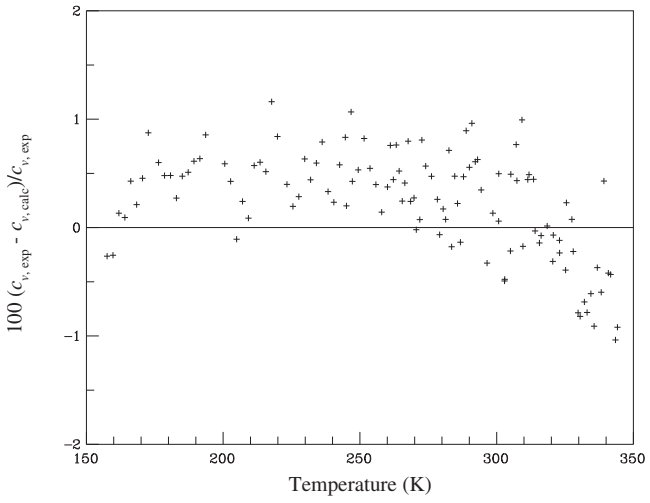

FIG. 18. Comparisons of isochoric heat capacities c_v calculated with the equation of state to experimental data as a function of temperature.

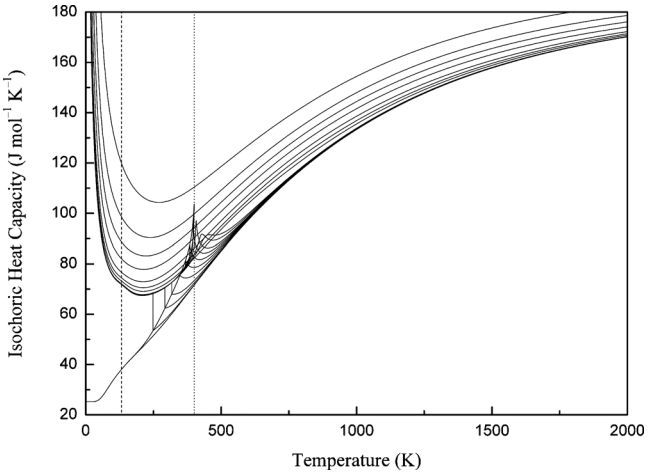

FIG. 19. Isochoric heat capacity c_v versus temperature. Isobars are shown at pressures of 0, 0.1, 0.5, 1, 2, 3, 4, 5, 6, 8, 10, 20, 50, 100, 200, 500, 1000, 2000, and 5000 MPa. The dashed line and the dotted line are shown at the triple-point temperature T_{tp}=131.66 K and the critical-point temperature T_c=400.378 K, respectively.

Figure 21 shows sound speed w versus temperature. The dashed line and the dotted line show the triple-point temperature T_{tp}=131.66 K and the critical-point temperature T_c=400.378 K, respectively. As shown in the figure, the saturated-liquid line remains straight down to about 50 K, a reduced temperature of 0.125, which is well below the triple-point temperature (the dashed line). The figure also shows that the extrapolation behavior to high temperatures and pressures is reasonable.

Figure 22 shows the density behavior along isobars of the equation of state for dimethyl ether. The rectilinear diameter is shown in the diagram, and is straight, as it should be, up to the critical point.

Figure 23 shows the isothermal behavior of the equation of state at extreme conditions of temperature and pressure.

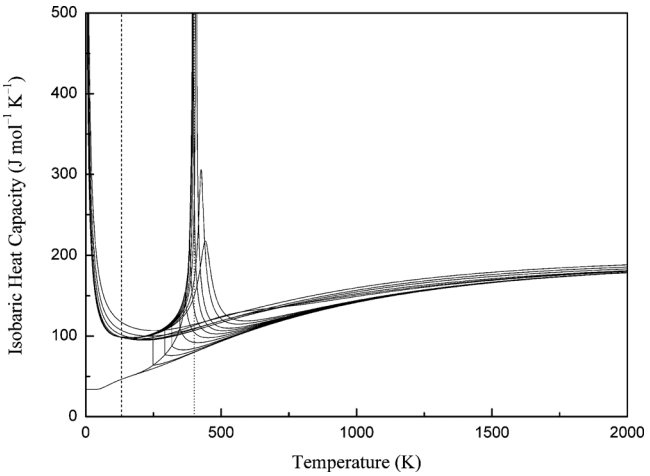

FIG. 20. Isobaric heat capacity c_p versus temperature. Isobars are shown at pressures of 0, 0.1, 0.5, 1, 2, 3, 4, 5, 6, 8, 10, 20, 50, 100, 200, 500, 1000, 2000, and 5000 MPa. The dashed line and the dotted line are shown at the triple-point temperature T_{tp}=131.66 K and the critical-point temperature T_c=400.378 K, respectively.

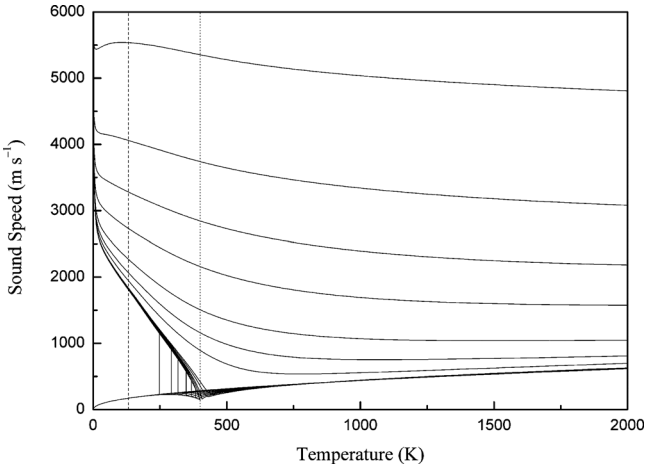

FIG. 21. Sound speed w versus temperature. Isobars are shown at pressures of 0, 0.1, 0.5, 1, 2, 3, 4, 5, 6, 8, 10, 20, 50, 100, 200, 500, 1000, 2000, and 5000 MPa. The dashed line and the dotted line are shown at the triple-point temperature T_{tp}=131.66 K and the critical-point temperature T_c=400.378 K, respectively.

The figure indicates that the extrapolation behavior to extremely high pressures, densities, and temperatures is reasonable. As explained by Lemmon and Jacobsen,[22] the smooth behavior comes from the term with t_i=1 and d_i=4.

Figure 24 shows the characteristic (ideal) curves of the equation of state as a function of reduced temperature T/T_c and reduced pressure p/p_c. Figure 24 is used to assess the behavior of the equation of state in regions without available experimental data.[23,24,30] The characteristic curves describe the behavior of the compressibility factor $Z \equiv p/\rho RT$ and include the Boyle curve, the Joule–Thomson inversion curve, the Joule inversion curve, and the ideal curve. The Boyle curve is given by

$$\left(\frac{\partial Z}{\partial v}\right)_T = 0. \tag{16}$$

The Joule–Thomson inversion curve is given by

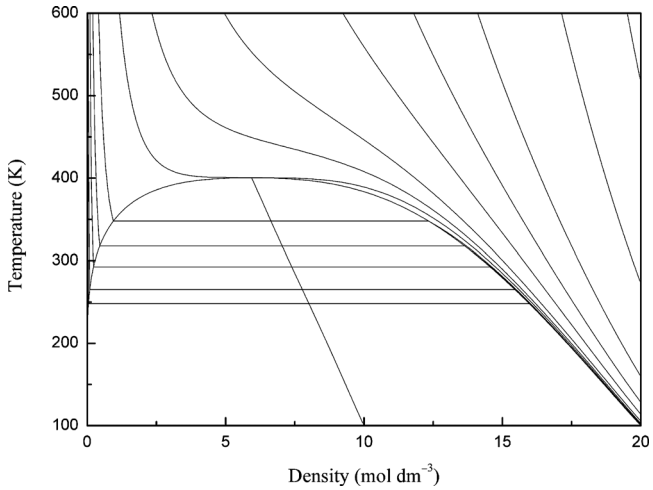

FIG. 22. Isobaric behavior of the equation of state for dimethyl ether. Isobars are shown at pressures of 0.1, 0.2, 0.5, 1, 2, p_c, 10, 20, 50, 100, 200, 500, and 1000 MPa. The rectilinear diameter is shown in the diagram.

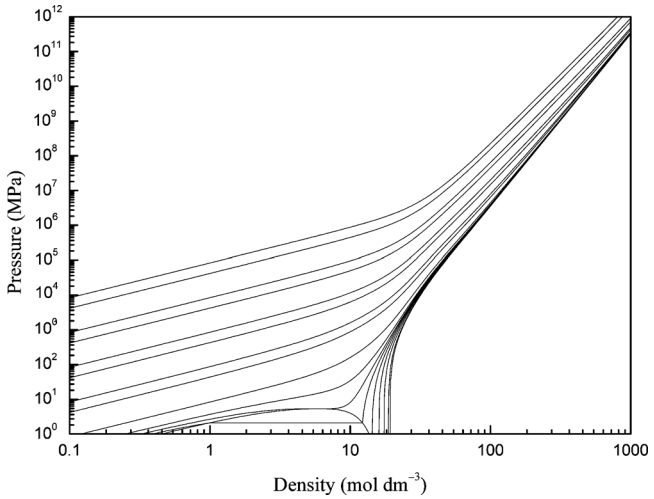

FIG. 23. Isothermal behavior of the equation of state at extreme conditions of temperature and pressure. Isotherms are shown at temperatures of T_{tp}, 150, 200, 250, 300, 350, T_c, 500, 1000, 5000, 10 000, 50 000, 100 000, 500 000, and 1 000 000 K.

$$\left(\frac{\partial Z}{\partial T}\right)_p = 0. \tag{17}$$

The Joule inversion curve is given by

$$\left(\frac{\partial Z}{\partial T}\right)_v = 0. \tag{18}$$

The ideal curve is given by

$$Z = \frac{p}{\rho RT} = 1. \tag{19}$$

Overall, these plots indicate that the equation-of-state behavior is appropriate within the valid range, and that the extrapolation behavior is reasonable at higher temperatures and pressures.

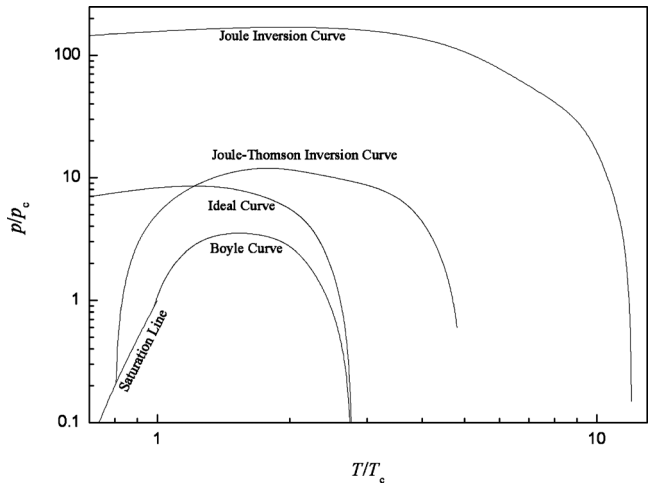

FIG. 24. Characteristic (ideal) curves of the equation of state as a function of reduced temperature T/T_c and reduced pressure p/p_c.

5. Conclusions

A new equation of state for dimethyl ether has been developed. The deviation in density is generally less than 0.1% and does not exceed 0.25% in the liquid region. In the supercritical region, the deviation in density is generally less than 0.25%, except for a few data points. The deviation in vapor pressure of the equation of state is generally less than 0.5%. The deviation in saturation heat capacity and isochoric heat capacity is generally less than 1.0%.

The uncertainties ($k=2$, indicating a level of confidence of 95%) of the equation of state in density are 0.1% in the liquid phase and 0.3% in the vapor phase. In the extended critical region, the uncertainty in density is 0.5%, except for very near the critical point. In the vapor-liquid region, the uncertainty in vapor pressure is 0.2% above 230 K, but increases as temperature decreases; the uncertainty in saturated liquid density is 0.05%, except for very near the critical point. The uncertainty in heat capacity is 2.0%.

The equation of state of this work is valid from the triple-point temperature to 550 K, with pressures up to 50 MPa, and densities up to 19 mol dm^{-3}. As detailed in this article, the extrapolation behavior of the equation of state is reasonable, and the equation can be extrapolated up to the dissociation limit of the fluid, with pressures up to 100 MPa. Ancillary equations for the vapor pressure and saturated liquid and vapor densities have also been developed that can be used for fast calculation or as the initial value for iteration with the equation of state.

There is a need for further measurement of caloric properties of dimethyl ether, including sound speed and heat capacity. Transport properties (such as viscosity and thermal conductivity) should be further measured to develop formulations for use in engineering system design and analysis.

6. Acknowledgments

This research is supported by the Foundation for the National Natural Science Foundation of China (Grant No. 51076128), the National High Technology Research and Development Program of China (Grant No. 2009AA05Z107), and the Fok Ying Tung Education Foundation (Project No. 111060).

7. References

[1] T. A. Semelsberger, R. L. Borup, and H. L. Greene, J. Power Sources **156**, 497 (2006).
[2] S. Bobbo, R. Camporese, and R. Stryjek, J. Chem. Thermodyn. **30**, 1041 (1998).
[3] J. T. Wu, Ph.D. thesis, Xi'an Jiaotong University, 2003.
[4] J. T. Wu, Z. G. Liu, S. S. Bi, and X. Y. Meng, J. Chem. Eng. Data **48**, 426 (2003).
[5] J. T. Wu, Z. G. Liu, J. Pan, and X. M. Zhao, J. Chem. Eng. Data **49**, 32 (2004).
[6] J. T. Wu, Z. G. Liu, B. Wang, and J. Pan, J. Chem. Eng. Data **49**, 704 (2004).
[7] J. T. Wu, Z. G. Liu, F. K. Wang, and C. Ren, J. Chem. Eng. Data **48**, 1571 (2003).
[8] J. T. Wu and J. W. Magee, 17th Symposium on Thermophysical Properties, Boulder, Colorado, USA, 2009.

[9] J. T. Wu, B. Wang, L. M. Yuan, and Z. G. Liu, J. Eng. Phys. Thermophys. **27**, 748 (2006).
[10] J. T. Wu and J. G. Yin, J. Chem. Eng. Data **53**, 2247 (2008).
[11] J. G. Yin and J. T. Wu, Fluid Phase Equilib. **298**, 298 (2010).
[12] E. C. Ihmels and E. W. Lemmon, Fluid Phase Equilib. **260**, 36 (2007).
[13] R. M. Kennedy, M. Sagenkahn, and J. G. Aston, J. Am. Chem. Soc. **63**, 2267 (1941).
[14] H. A. Duarte-Garza and J. W. Magee, Int. J. Thermophys. **18**, 173 (1997).
[15] W. Wagner, Cryogenics **13**, 470 (1973).
[16] O. Maass and E. H. Boomer, J. Am. Chem. Soc. **44**, 1709 (1922).
[17] J. A. Nelder and R. Mead, Comput. J. **7**, 308 (1965).
[18] R. Span, *Multiparameter Equations of State—An Accurate Source of Thermodynamic Property Data* (Springer, Berlin, 2000).
[19] R. T. Jacobsen, S. G. Penoncello, and E. W. Lemmon, in *Experimental Thermodynamics*, edited by J. V. Sengers, R. F. Kayser, and C. J. Peters (Elsevier, Amsterdam, 2000), Vol. 5, p. 35.
[20] P. J. Mohr, B. N. Taylor, and D. B. Newell, Rev. Mod. Phys. **80**, 633 (2008).
[21] U. Setzmann and W. Wagner, J. Phys. Chem. Ref. Data **20**, 1061 (1991).
[22] E. W. Lemmon and R. T. Jacobsen, J. Phys. Chem. Ref. Data **34**, 68 (2005).
[23] E. W. Lemmon, M. O. McLinden, and W. Wagner, J. Chem. Eng. Data **54**, 3141 (2009).
[24] R. Span and W. Wagner, Int. J. Thermophys. **18**, 1415 (1997).
[25] S. L. Outcalt and M. O. McLinden, Ind. Eng. Chem. Res. **46**, 8264 (2007).
[26] A. Arteconi, G. D. Nicola, M. Moglie, G. Santori, and R. Stryjek, J. Therm Anal. Calorim. **97**, 631 (2009).
[27] A. Arteconi, G. D. Nicola, G. Santori, and R. Stryjek, J. Chem. Eng. Data **54**, 1840 (2009).
[28] E. G. Richardson and R. I. Tait, Philos. Mag. **2**, 441 (1957).
[29] K. Tanaka and Y. Higashi, J. Chem. Eng. Data **55**, 2658 (2010).
[30] U. K. Deiters and K. M. de Reuck, Pure Appl. Chem. **69**, 1237 (1997).
[31] A. Nadezhdin, Beibl. Ann. Phys. **7**, 678 (1883).
[32] A. Leduc and P. Sacerdote, Seances Acad. Sci. **125**, 397 (1897).
[33] E. Briner and E. Cardoso, Seances Acad. Sci. **144**, 911 (1907).
[34] E. Briner and E. Cardoso, J. Chim. Phys. Phys.-Chim. Biol. **6**, 641 (1908).
[35] E. Cardoso and A. Bruno, J. Chim. Phys. Phys.-Chim. Biol. **20**, 347 (1923).
[36] E. Cardoso and A. A. Coppola, J. Chim. Phys. Phys.-Chim. Biol. **20**, 337 (1923).
[37] C. A. Winkler and O. Maass, Can. J. Res. **6**, 458 (1932).
[38] C. A. Winkler and O. Maass, Can. J. Res. **9**, 613 (1933).
[39] J. S. Tapp, E. W. R. Steacie, and O. Maass, Can. J. Res. **9**, 217 (1933).
[40] J. Edwards and O. Maass, Can. J. Res., Sect. A **12**, 357 (1935).
[41] D. B. Pall and O. Maass, Can. J. Res., Sect. B **14**, 96 (1936).
[42] B. Osipiuk and R. Stryjek, Bull. Acad. Pol. Sci., Ser. Sci. Chim. **18**, 289 (1970).
[43] A. C. Zawisza and S. Glowka, Bull. Acad. Pol. Sci., Ser. Sci. Chim. **18**, 549 (1970).
[44] J. R. Noles and J. A. Zollweg, Fluid Phase Equilib. **66**, 275 (1991).
[45] J. R. Noles and J. A. Zollweg, J. Chem. Eng. Data **37**, 306 (1992).
[46] A. P. Kudchadker, D. Ambrose, and C. Tsonopoulos, J. Chem. Eng. Data **46**, 457 (2001).
[47] M. Yasumoto, Y. Uchida, K. Ochi, T. Furuya, and K. Otake, J. Chem. Eng. Data **50**, 596 (2005).
[48] S. Glowka, Bull. Acad. Pol. Sci., Ser. Sci. Chim. **20**, 163 (1972).
[49] C. Y. Tsang and W. B. Streett, J. Chem. Eng. Data **26**, 155 (1981).
[50] E. Chang, J. C. G. Calado, and W. B. Streett, J. Chem. Eng. Data **27**, 293 (1982).
[51] H. Preuss and K. Moerke, Leuna Protocol, 1984, p. 11141.
[52] J. C. G. Calado, L. P. N. Rebelo, W. B. Streett, and J. A. Zollweg, J. Chem. Thermodyn. **18**, 931 (1986).
[53] H. Holldorff and H. Knapp, Fluid Phase Equilib. **40**, 113 (1988).
[54] H. Preuss, D. Pape, and S. Stoeck, Leuna Protocol, 1991, p. 6041.
[55] M. E. Pozo de Fernandez, J. C. G. Calado, J. A. Zollweg, and W. B. Streett, Fluid Phase Equilib. **74**, 289 (1992).
[56] T. Tsujimoto, H. Kubota, Y. Tanaka, S. Matsuo, and T. Sotani, 13th Japan Symposium on Thermophysical Properties, Tokyo, Japan, 1992.
[57] A. Jonasson, O. Persson, and P. Rasmussen, J. Chem. Eng. Data **40**, 1209 (1995).
[58] A. Jonasson, O. Persson, and A. Fredenslund, J. Chem. Eng. Data **40**, 296 (1995).
[59] S. Bobbo, R. Camporese, R. Stryjek, and S. K. Malanowski, J. Chem. Eng. Data **45**, 829 (2000).
[60] S. Bobbo, L. Fedele, R. Camporese, and R. Stryjek, Fluid Phase Equilib. **174**, 3 (2000).
[61] N. F. Giles and G. M. Wilson, J. Chem. Eng. Data **45**, 146 (2000).
[62] M. Teodorescu and P. Rasmussen, J. Chem. Eng. Data **46**, 640 (2001).
[63] L. J. Florusse, T. Fornari, S. B. Bottini, and C. J. Peters, J. Supercrit. Fluids **22**, 1 (2002).
[64] S. Bobbo, L. Fedele, R. Camporese, and R. Stryjek, Fluid Phase Equilib. **199**, 153 (2002).
[65] T. Laursen, P. Rasmussen, and S. I. Andersen, Can. J. Chem. **47**, 198 (2002).
[66] H. Daiguji and E. Hihara, J. Chem. Eng. Data **48**, 266 (2003).
[67] S. Bobbo, L. Fedele, M. Scattolini, R. Camporese, and R. Stryjek, Fluid Phase Equilib. **224**, 119 (2004).
[68] S. Bobbo, M. Scattolini, L. Fedele, and R. Camporese, J. Chem. Eng. Data **50**, 1667 (2005).
[69] L. Fedele, S. Bobbo, V. D. Stefani, R. Camporese, and R. Stryjek, J. Chem. Eng. Data **50**, 128 (2005).
[70] A. Valtz, L. Gicquel, C. Coquelet, and D. Richon, Fluid Phase Equilib. **230**, 184 (2005).
[71] F. Corvaro, G. D. Nicola, F. Polonara, and G. Santori, J. Chem. Eng. Data **51**, 1469 (2006).
[72] J. Im, G. Lee, J. Lee, and H. Kim, J. Chem. Thermodyn. **38**, 1510 (2006).
[73] J. Im, G. Lee, J. Lee, and H. Kim, Fluid Phase Equilib. **251**, 59 (2007).
[74] S.-J. Park, K.-J. Han, and J. Gmehling, J. Chem. Eng. Data **52**, 1814 (2007).
[75] A. V. Grosse, R. C. Wackher, and C. B. Linn, J. Phys. Chem. **44**, 275 (1940).
[76] R. D. Mallemann, F. Sunner, and A. Malevergne, Seances Acad. Sci. **232**, 1385 (1951).
[77] T. B. Tripp and R. D. Dunlap, J. Phys. Chem. **66**, 635 (1962).
[78] K. P. Lawley and L. E. Sutton, Trans. Faraday Soc. **59**, 2680 (1963).
[79] W. S. Haworth and L. E. Sutton, Trans. Faraday Soc. **67**, 2907 (1971).
[80] L. Wu, C. Wang, X. Hu, H. Li, and S. J. Han, J. Chem. Thermodyn. **38**, 889 (2006).
[81] W. Cawood and H. S. Patterson, J. Chem. Soc. **33**, 619 (1933).
[82] T. B. Tripp, M.S. thesis, University of Maine, 1961.
[83] S. K. K. Jatkar, J. Indian Inst. Sci. Sec. A Sci. **22**, 19 (1939).
[84] G. B. Kistiakowsky and W. W. Rice, J. Chem. Phys. **8**, 618 (1940).
[85] M. Miyazaki, H. Kubota, Y. Tanaka, and S. Matsuo, 12th Japan Symposium on Thermophysical Properties, Tokyo, Japan, 1991.